

Spatio-temporal images of growth-factor-induced activation of Ras and Rap1

Naoki Mochizuki*, Shigeko Yamashita†, Kazuo Kurokawa‡, Yusuke Ohba‡, Takeharu Nagai§, Atsushi Miyawaki§ & Michiyuki Matsuda‡

* Department of Structural Analysis, National Cardiovascular Center Research Institute, 5-7-1 Fujishirodai, Suita-shi, Osaka 565-8565, Japan

† Department of Pathology, Research Institute, International Medical Center of Japan, 1-21-1 Toyama, Shinjuku-ku, Tokyo 162-8655, Japan

‡ Department of Tumor Virology, Institute for Microbial Diseases, Osaka University, 3-1 Yamadaoka, Suita-shi, Osaka 565-0871, Japan

§ Laboratory for Cell Function and Dynamics, Brain Science Institute, RIKEN, 2-1 Hirosawa, Wako-shi, Saitama 351-0198, Japan

G proteins of the Ras family function as molecular switches in many signalling cascades^{1–3}; however, little is known about where they become activated in living cells. Here we use FRET (fluorescent resonance energy transfer)-based sensors to report on the spatio-temporal images of growth-factor-induced activation of Ras and Rap1. Epidermal growth factor activated Ras at the peripheral plasma membrane and Rap1 at the intracellular perinuclear region of COS-1 cells. In PC12 cells, nerve growth factor-induced activation of Ras was initiated at the plasma membrane and transmitted to the whole cell body. After three hours, high Ras activity was observed at the extending neurites. By using the FRAP (fluorescence recovery after photobleaching) technique, we found that Ras at the neurites turned over rapidly; therefore, the

sustained Ras activity at neurites was due to high GTP/GDP exchange rate and/or low GTPase activity, but not to the retention of the active Ras. These observations may resolve long-standing questions as to how Ras and Rap1 induce different cellular responses⁴ and how the signals for differentiation and survival are distinguished by neuronal cells⁵.

G proteins of the Ras family cycle between GDP-bound inactive and GTP-bound active forms. This cycle is regulated by guanine nucleotide exchange factor (GEF), the activator, and GTPase activating protein (GAP), the inactivator. Many external and internal signals converge on G proteins of the Ras family through several GEFs and GAPs; however, if so many signals can activate G proteins of the Ras family, it remains unknown how they transmit a specific signal^{4,6}.

After making a calcium indicator based on FRET technology⁷, we designed a protein that consisted of H-Ras, the Ras-binding domain of Raf (RafRBD) and a pair of an enhanced yellow-emitting mutant of green fluorescent protein (YFP) and an enhanced cyan-emitting mutant of green fluorescent protein (CFP), so that intramolecular binding of GTP-Ras to Raf RBD brings CFP close to YFP and increases FRET between CFP and YFP (Fig. 1a). This protein was named a Ras and interacting protein chimaeric unit (Raichu). By replacing Ras with Rap1, we also made a probe for Rap1. Raichu-Ras and Raichu-Rap1 were co-expressed in 293T cells with either GEFs or GAPs, and their emission profiles were examined with an excitation wavelength of 433 nm (Fig. 1b). FRET, which was typically observed as an emission peak of 527 nm, was more prominent in the presence of GEFs than in the presence of GAPs. After treatment with proteinase K, which cleaved Raichu-Ras and Raichu-Rap1 between YFP and CFP, the emission peak at 527 nm disappeared, proving that this peak was caused by FRET⁸.

To correlate GTP loading with FRET efficiency, we labelled cells expressing Raichu-Ras, Flag-tagged H-Ras and a varying quantity

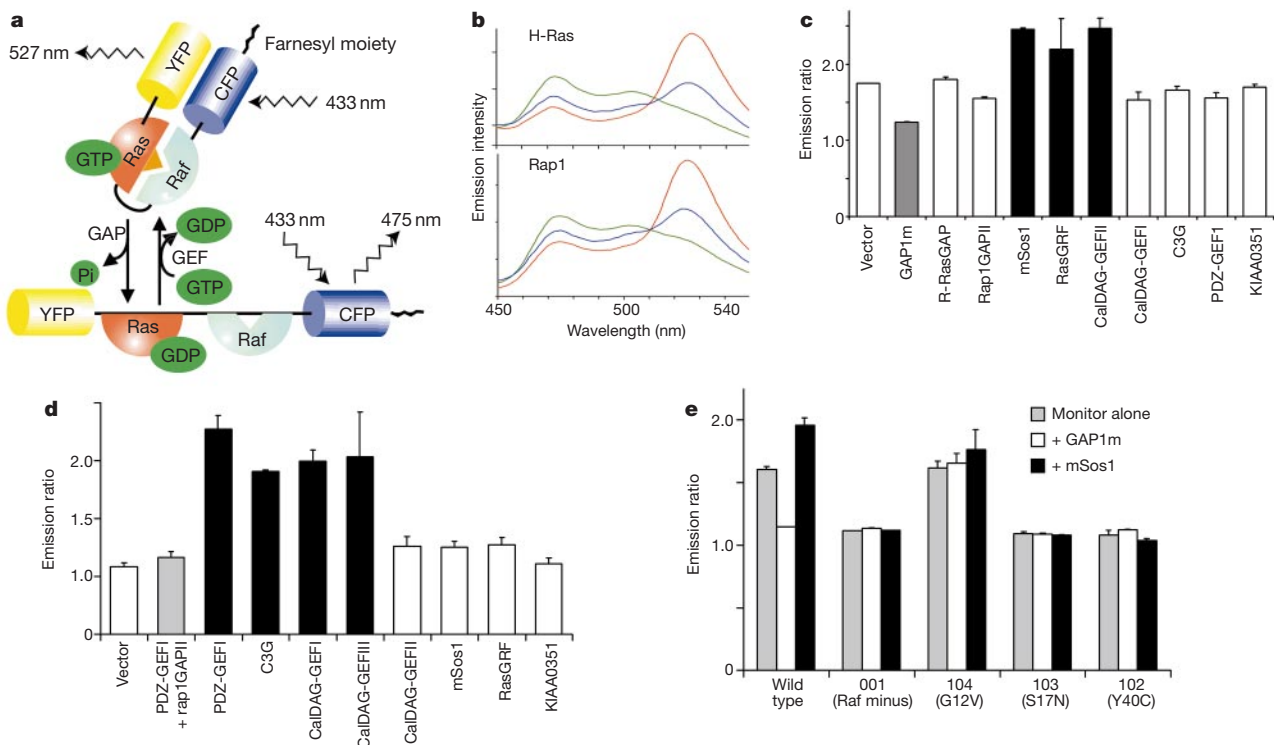


Figure 1 Properties of Raichu-Ras and Raichu-Rap1. **a**, Schematic representation of Raichu-Ras bound to GDP or GTP. **b**, Emission spectra of Raichu-Ras and Raichu-Rap1 (excited at 433 nm) co-expressed with GEF (red) or GAP (blue) in 293T cells. To confirm FRET, one sample was treated with proteinase K (green), which cleaved Raichu between

CFP and YFP. **c, d**, Emission ratio of Raichu-Ras or Raichu-Rap1 co-expressed with GAPs and GEFs in 293T cells. GAPs and GEFs for Ras (**c**) or Rap1 (**d**) are indicated in grey and black columns, respectively. **e**, Emission ratio of Raichu-Ras mutants expressed with or without GAP1m or mSos1 in 293T cells. Bars are s.d. ($n = 3$).

of either mSos1 or GAP1m with $^{32}\text{P}_i$ and determined the amount of GTP bound to Raichu-Ras and Flag-tagged H-Ras by thin layer chromatography (see Supplementary Information Fig. 1). FRET efficiency, which is shown as an emission ratio of 527/475 nm, correlated well with the amount of GTP bound to Raichu-Ras. The percentage of GTP-bound Raichu-Ras was always higher than that of GTP-bound Flag-H-Ras obtained from the same cells. This is probably because Raf RBD present on Raichu-Ras competitively inhibits GAP⁹. Despite this, the linear correlation of GTP-loading and FRET efficiency and the large dynamic range of the emission ratio from 1.2 to 2.4 show that Raichu-Ras can be used for monitoring Ras activation *in vivo*. Similar results were obtained for Raichu-Rap1.

We next tested the specificity of Raichu-Ras on a panel of GEFs and GAPs of G proteins of the Ras family (Fig. 1c). Neither R-RasGAP, which is related closely to GAP1m but specific to R-Ras, nor rap1GAPII, a GAP for Rap1, stimulated the GTPase activity of Raichu-Ras. RasGRF and CalDAG-GEFII, GEFs for Ras and R-Ras, increased FRET, as did mSos1. In contrast, GEFs for Rap1, R-Ras or Ral including CalDAG-GEFI, C3G, PDZ-GEFI and KIAA0351 (RalGPS/RalGEF2) did not show any effect on the FRET efficiency of Raichu-Ras. Thus, Raichu-Ras retained specificity for both GEFs and GAPs of the classical Ras subfamily. Again, similar results were obtained for Raichu-Rap1 (Fig. 1d): the emission ratio of Raichu-Rap1 was increased in the presence of GEFs for Rap1 including PDZ-GEFI, C3G, CalDAG-GEFI and CalDAG-GEFIII, and was decreased in the presence of GAPs for G proteins of the Rap family including rap1GAPII and Spa1 (see Supplementary Information Fig. 2).

To confirm that the increased emission ratio of Raichu-Ras was caused by the intramolecular binding of Ras to Raf RBD, we constructed a series of mutants: Raichu 001 lacked Raf RBD; Raichu 103 contained an S17N mutation in Ras, which reduced the affinity to guanine nucleotides¹⁰; and Raichu 102 contained a Y40C mutation in which the interaction of H-Ras with Raf was abolished¹¹. In these mutants, the FRET efficiency was not enhanced

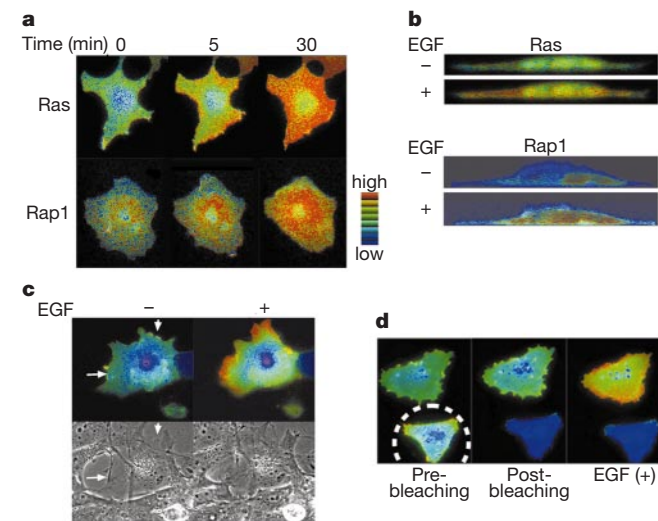


Figure 2 EGF activation of Ras and Rap1. **a**, IMD images of COS-1 cells expressing Raichu-Ras or Raichu-Rap1 and stimulated by EGF. **b**, Tangential IMD images obtained with a confocal microscope. COS-1 cell expressing Raichu-Ras or Raichu-Rap1 were stimulated by EGF for 5 min. **c**, Phase contrast and IMD images of a Raichu-Ras-expressing COS-1 cell, which had grown to subconfluency and was stimulated by EGF for 5 min. Arrows indicate the free edge of the cell, to which Ras activation was restricted. **d**, Cell indicated by a dotted line (left) was photobleached at an excitation wavelength of 510 nm for 2 min (centre) and stimulated by EGF for 5 min (right).

in the presence of mSos1 (Fig. 1e). Raichu 104, which lacked GTPase activity because of a G12V mutation in Ras², had an increased FRET efficiency irrespective of the presence of GAP1m or mSos1. Thus, the effects of mutations shown either to inhibit or to activate H-Ras were reproduced upon mutation of Raichu-Ras.

Because the effector domain of the GTP-loaded Raichu is occupied by Raf RBD, Raichu will not perturb the cellular signalling cascades by binding to the cellular target proteins. In fact, we confirmed that expression of Raichu-Ras and Raichu-Rap1 neither enhanced nor attenuated the epidermal growth factor (EGF)-induced ERK/MAPK activation (see Supplementary Information Fig. 3).

With these probes, we monitored the activation of Ras and Rap1 in living COS-1 cells by a dual-emission ratio fluorescent microscopy. CFP and YFP images were taken every 20 s and used to create FRET images (see Supplementary Information movie 1). In the following figures, the FRET images are presented in intensity-modulated display (IMD) mode, which associates colour hue with emission ratio value and the intensity of each hue with the source image brightness. We found that EGF-induced Ras activation was marked at the periphery of the cells, where membrane ruffling was prominent (Fig. 2a and Supplementary Information movie 2). In contrast, EGF activated Rap1 mostly in the centre of the cells (Fig. 2a and Supplementary Information movie 2). Use of a confocal microscope showed more clearly that, upon EGF stimulation, Ras activity increased mostly at the peripheral plasma membrane (Fig. 2b). However, EGF activated Rap1 at the internal perinuclear region of the cells, but not at the plasma membrane. EGF did not stimulate a Raichu-Rap1 mutant that lacked a farnesyl moiety,

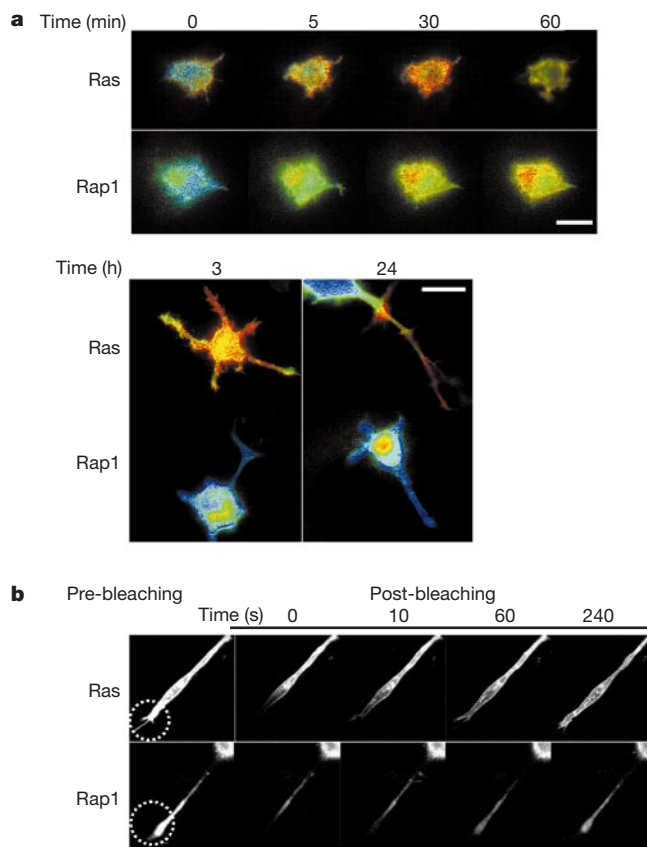


Figure 3 Activation of Ras and Rap1 in NGF-stimulated PC12 cells. **a**, IMD images of PC12 cells expressing Raichu-Ras or Raichu-Rap1 and stimulated by NGF. Scale bars, 10 μm . **b**, Neurites of differentiated PC12 cells expressing YFP-Ras or YFP-Rap1 after they were photobleached.

indicating that Rap1 was activated at the intracellular membrane compartments. When we pretreated cells with monodansylcadaverine, an inhibitor for clathrin-mediated endocytosis, EGF activated Ras, but not Rap1. Therefore, only the internalized EGF receptor may activate C3G, a Rap1 GEF activated by tyrosine phosphorylation¹².

When subconfluent COS-1 cells were stimulated with EGF, Ras was activated mostly at the free edge of the cells, but less at the edge in contact with the neighbouring cells, where membrane ruffling was suppressed (Fig. 2c). It is proposed that GAP activity is increased in confluent cells¹³. Our observation indicates that local activation of GAP at the sites of cell-to-cell contact may attenuate Ras activation.

The EGF-induced increase in FRET was not observed in Raichu-102 (Y40C mutant)-expressing cells, in cells co-expressing Raichu-Ras with a dominant negative mutant of H-Ras (S17N) (see Supplementary Information movie 3) or in cells pretreated with AG1478, a tyrosine kinase inhibitor. To confirm that the increase in the emission ratio of YFP to CFP was due to FRET, we photobleached one of a pair of Raichu-Ras-expressing cells on YFP before EGF stimulation⁸. As expected, only the non-photobleached cells had an increased emission ratio upon EGF stimulation (Fig. 2d).

We next examined the activation of Ras and Rap1 in the rat pheochromocytoma cell line PC12. Upon nerve growth factor (NGF) stimulation, Ras was activated from the periphery of the PC12 cells (Fig. 3a). Within 3 h, Ras activation diminished in the cell body and became apparent in the extending neurites. After 24 h, when PC12 cells differentiated into neuronal cells, activation of Ras persisted only in the extended neurites. Again, in contrast to Ras, Rap1 was activated at the intracellular region of NGF-stimulated PC12 cells, but never at the neurites. It has been proposed that differentiation of the PC12 cells is prompted by the NGF receptor (TrkA) at the endosomes and that survival responses are initiated by TrkA at the cell surface¹⁴. This is consistent with our observation that Ras is activated transiently at the cell body and persistently at the extended neurites. The high Ras activity at the neurites may be maintained by the NGF-TrkA complex, which is transported from the axon to the cells and is required for ERK-dependent phosphorylation of CREB cyclic AMP response element-binding protein¹⁵.

To understand the mechanism underlying the intracellular gradient of the activities of Ras and Rap1, the mobility of Ras and Rap1 was examined by FRAP¹⁶. We photobleached neurites of the PC12 cells expressing YFP-Ras or YFP-Rap1 and monitored the recovery of fluorescence intensity (Fig. 3b). In both cells, the fluorescence intensity recovered within 240 s. This observation indicates that the sustained high activity of Ras and low activity of Rap1 were not caused by the retention of active Ras or inactive Rap1 at the neurites. It is likely that local balance between the activities of GEFs and GAPs determines the local activities of Ras and Rap1.

Rap1 antagonizes Ras-dependent cellular transformation and ERK activation in some cell types^{17,18}, probably by sequestering the Ras-Raf complex¹⁹. We have found that, upon growth factor activation, the localizations of the active Ras and active Rap1 are exclusive of each other. Moreover, expression of active Rap1, Rap1V12, did not inhibit EGF-induced Ras activation (see Supplementary Information movie 3). Therefore, it is unlikely that activated Rap1 inhibits the Ras-dependent ERK activation by trapping the Ras-Raf complex. However, Rap1 may attenuate Ras-dependent activation of ERK by retaining Raf in the perinuclear region and reducing the quantity of Raf at the plasma membrane. This view is supported by the observation that overexpression of rap1GAP enhanced growth-factor-induced ERK activation²⁰.

Previous biochemical analyses rarely detected more than 40% activation of Ras and Rap1 upon growth factor stimulation²¹. It has now become clear that growth-factor stimulation strongly activates Ras and Rap1 in a very restricted area within cells, and that a large

population of Ras or Rap1 remains inactive, causing an apparent low-level response in biochemical assays. Thus, the probes reported here enable highly sensitive monitoring of the activities of Ras and Rap1 with spatio-temporal information. This property also promises the widespread application of this probe *in vivo*. □

Methods

For detailed methods, see Supplementary Information.

Plasmids

pRaichu-Ras was derived from the pCAGGS eukaryotic expression vector²² and encoded a chimaeric protein, Raichu-Ras, which consisted of EYFP-V68L/Q69K²³, H-Ras, Raf RBD and ECFP from the amino terminus. In pRaichu-Rap1, H-Ras was replaced with Rap1A. The nucleotide sequences of the coding regions of pRaichu-Ras and pRaichu-Rap1 were deposited in the DDBJ/EMBL/GenBank data (accession nos AB046925 and AB051846). Plasmids used in this study have been described previously²⁴.

Cells and Imaging

COS-1 and PC12 cells were plated on a collagen-coated 35-mm-diameter glass-base dish (Asahi Techno Glass), transfected with plasmids, starved of serum for 6 h, and stimulated with 5 ng ml⁻¹ EGF or 25 ng ml⁻¹ NGF. In some experiments, cells were pretreated with 10 nM AG1478 (Calbiochem) for 30 min or 20 μM monodansylcadaverine (Sigma) for 10 min. Dual-emission ratio imaging and FRAP experiments were performed as described elsewhere^{7,25}.

Received 7 December 2000; accepted 26 March 2001.

1. Barbacid, M. *ras* genes. *Annu. Rev. Biochem.* **56**, 779–827 (1987).
2. Lowy, D. R. & Willumsen, B. M. Function and regulation of *ras*. *Annu. Rev. Biochem.* **62**, 851–891 (1993).
3. Schlessinger, J. & Bar-Sagi, D. Activation of *ras* and other signaling pathways by receptor tyrosine kinases. *Cold Spring Harb. Symp. Quant. Biol.* **59**, 173–179 (1994).
4. Bos, J. L. All in the family? New insights and questions regarding interconnectivity of Ras, Rap1 and Ral. *EMBO J.* **17**, 6776–6782 (1998).
5. Marshall, C. J. Specificity of receptor tyrosine kinase signaling: transient versus sustained extracellular signal-regulated kinase activation. *Cell* **80**, 179–185 (1995).
6. Vojtek, A. B. & Der, C. J. Increasing complexity of the Ras signaling pathway. *J. Biol. Chem.* **273**, 19925–19928 (1998).
7. Miyawaki, A. *et al.* Fluorescent indicators for Ca²⁺ based on green fluorescent proteins and calmodulin. *Nature* **388**, 882–887 (1997).
8. Miyawaki, A. & Tsien, R. Y. Monitoring protein conformations and interactions by fluorescence resonance energy transfer. *Methods Enzymol.* **327**, 472–500 (2000).
9. Scheffler, J. E. *et al.* Characterization of a 78-residue fragment of c-Raf-1 that comprises a minimal binding domain for the interaction with Ras-GTP. *J. Biol. Chem.* **269**, 22340–22346 (1994).
10. Feig, L. A. & Cooper, G. M. Inhibition of NIH3T3 cell proliferation by a mutant *ras* protein with preferential affinity for GDP. *Mol. Cell. Biol.* **8**, 3235–3243 (1988).
11. Rodriguez-Viciana, P. *et al.* Role of phosphoinositide 3-OH kinase in cell transformation and control of the actin cytoskeleton by Ras. *Cell* **89**, 457–467 (1997).
12. Ichiba, T. *et al.* Activation of C3G guanine nucleotide exchange factor for Rap1 by phosphorylation of tyrosine 504. *J. Biol. Chem.* **274**, 14376–14381 (1999).
13. Hoshino, M., Kawakita, M. & Hattori, S. Characterization of a factor that stimulates hydrolysis of GTP bound to *ras* gene product p21 (GTPase-activating protein) and correlation of its activity to cell density. *Mol. Cell. Biol.* **8**, 4169–4173 (1988).
14. Zhang, Y., Moheban, D. B., Conway, B. R., Bhattacharyya, A., & Segal, R. A. Cell surface Trk receptors mediate NGF-induced survival while internalized receptors regulate NGF-induced differentiation. *J. Neurosci.* **20**, 5671–5678 (2000).
15. Riccio, A., Pierchala, B. A., Ciarallo, C. L. & Ginty, D. D. An NGF-TrkA-mediated retrograde signal to transcription factor CREB in sympathetic neurons. *Science* **277**, 1097–1100 (1997).
16. Xing, J., Kornhauser, J. M., Xia, Z., Thiele, E. A. & Greenberg, M. E. Nerve growth factor activates extracellular signal-regulated kinase and p38 mitogen-activated protein kinase pathways to stimulate CREB serine 133 phosphorylation. *Mol. Cell Biol.* **18**, 1946–1955 (1998).
17. Kitayama, H., Sugimoto, Y., Matsuzaki, T., Ikawa, Y. & Noda, M. A *ras*-related gene with transformation suppressor activity. *Cell* **56**, 77–84 (1989).
18. Cook, S. J., Rubinfeld, B., Albert, I. & McCormick, F. RapV12 antagonizes Ras-dependent activation of ERK1 and ERK2 by LPA and EGF in Rat-1 fibroblasts. *EMBO J.* **12**, 3475–3485 (1993).
19. Hu, C. D. *et al.* Coassociation of Rap1A and Ha-Ras with Raf-1 N-terminal region interferes with Ras-dependent activation of Raf-1. *J. Biol. Chem.* **272**, 11702–11705 (1997).
20. Mochizuki, N. *et al.* Activation of ERK/MAPK pathway by an isoform of rap1GAP associated with G_{ai}. *Nature* **400**, 891–894 (1999).
21. Satoh, T., Nakafuku, M. & Kaziro, Y. Function of Ras as a molecular switch in signal transduction. *J. Biol. Chem.* **267**, 24149–24152 (1992).
22. Niwa, H., Yamamura, K. & Miyazaki, J. Efficient selection for high-expression transfectants with a novel eukaryotic vector. *Gene* **108**, 193–200 (1991).
23. Miyawaki, A., Griesbeck, O., Heim, R. & Tsien, R. Y. Dynamic and quantitative Ca²⁺ measurements using improved cameleons. *Proc. Natl Acad. Sci. USA* **96**, 2135–2140 (1999).
24. Ohba, Y. *et al.* Rap2 as a slowly responding molecular switch in the Rap1 signaling cascade. *Mol. Cell Biol.* **20**, 6074–6083 (2000).
25. Lippincott-Schwartz, J. *et al.* Monitoring the dynamics and mobility of membrane proteins tagged with green fluorescent protein. *Methods Cell Biol.* **58**, 261–281 (1999).

Supplementary information is available on Nature's World-Wide Web site (<http://www.nature.com>) or as paper copy from the London editorial office of Nature.

Acknowledgements

We thank D. Bowtell, K. Kaibuchi, J. Miyazaki, N. Minato and N. Nomura for plasmids; H. Mizuno, F. Ohba, N. Otsuka, K. Kimura and K. Okuda for technical assistance; and S. Hattori, M. Dutta and A. Dutta for the critical reading of the manuscript. Supported by grants from the Ministry of Health and Welfare, from the Ministry of Education, Science, Sports and Culture, Mitsui Life Social Welfare Foundation, the Princess Takamatsu Cancer Research Fund and from the Japan Health Science Foundation.

Correspondence and requests for materials should be addressed to M.M. (e-mail: matsudam@biken.osaka-u.ac.jp).

Cyclin-dependent kinases prevent DNA re-replication through multiple mechanisms

Van Q. Nguyen*, Carl Co* & Joachim J. Li†

* Department of Biochemistry and Biophysics; and † Department of Microbiology and Immunology, University of California, San Francisco, California 94143-0414, USA

The stable propagation of genetic information requires that the entire genome of an organism be faithfully replicated once and only once each cell cycle. In eukaryotes, this replication is initiated at hundreds to thousands of replication origins distributed over

the genome, each of which must be prohibited from re-initiating DNA replication within every cell cycle. How cells prevent re-initiation has been a long-standing question in cell biology. In several eukaryotes, cyclin-dependent kinases (CDKs) have been implicated in promoting the block to re-initiation¹, but exactly how they perform this function is unclear. Here we show that B-type CDKs in *Saccharomyces cerevisiae* prevent re-initiation through multiple overlapping mechanisms, including phosphorylation of the origin recognition complex (ORC), downregulation of Cdc6 activity, and nuclear exclusion of the Mcm2-7 complex. Only when all three inhibitory pathways are disrupted do origins re-initiate DNA replication in G2/M cells. These studies show that each of these three independent mechanisms of regulation is functionally important.

The mechanism of eukaryotic replication initiation and the role of CDKs in its regulation have been most extensively characterized in the budding yeast *S. cerevisiae* (reviewed in ref. 1). Initiation events at yeast origins can be divided into two fundamental stages: the assembly of pre-replicative complexes (pre-RCs) and the triggering of new DNA synthesis. The assembly of pre-RCs occurs shortly after mitosis and renders origins competent to initiate DNA synthesis. During this assembly ORC, which binds origins throughout the cell cycle, is joined by additional initiator proteins, including Cdc6 and the Mcm2-7 complex. Passage through the G1 commitment point (Start) then activates the kinases Cdc7-Dbf4 and the B-type CDKs Clb-Cdc28, which together trigger origin unwinding, assembly of the replication fork machinery, initiation of daughter strand synthesis, and pre-RC disassembly.

In addition to triggering initiation, Clb-Cdc28 prevents re-initiation, in part by blocking re-assembly of pre-RCs¹. This block

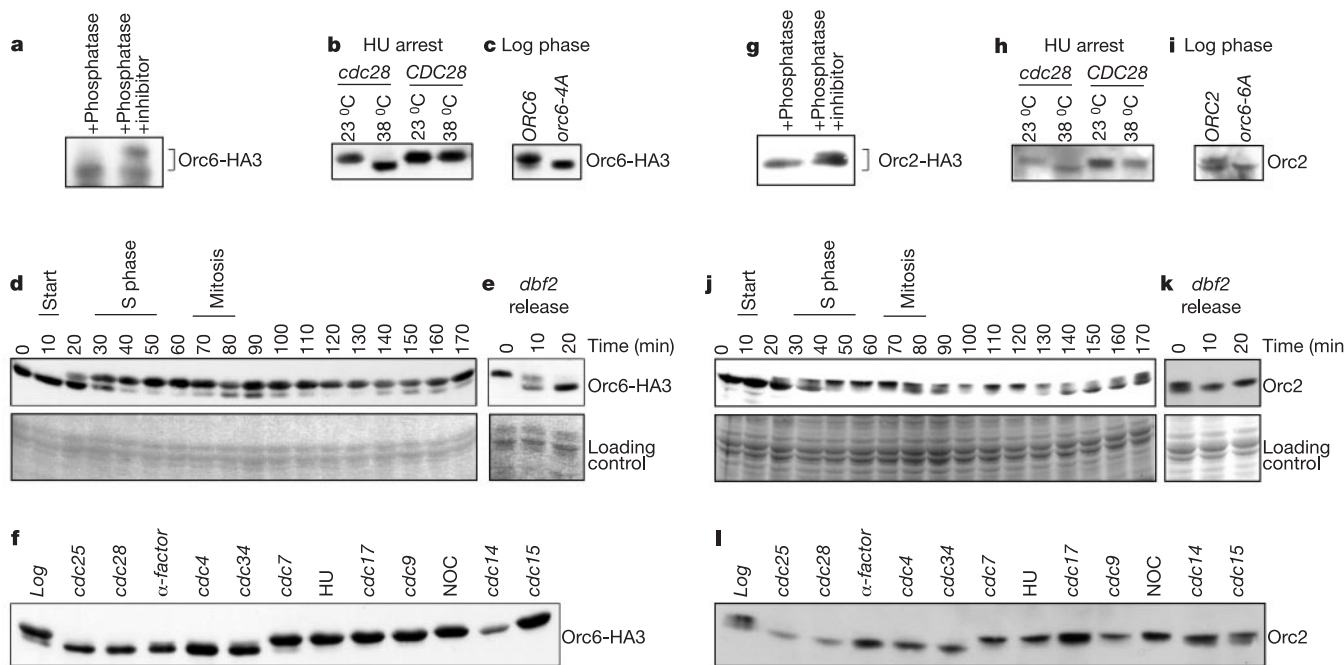


Figure 1 Clb-Cdc28 phosphorylation of Orc6 and Orc2 *in vivo*. **a–f**, Immunoblot of Orc6 using anti-haemagglutinin (HA) detection of Orc6-HA3 (**a–d, f**) or anti-Orc6 (**e**). **g–l**, Immunoblot of Orc2 using anti-HA detection of Orc2-HA3 (**g**) or anti-Orc2 (**h–l**). Extracts used in **h, j–l** were identical to those used in **b, d–f**, respectively. **a, g**, Immunoprecipitates from YJL921 (*ORC6-HA3*) (**a**) or YJL963 (*ORC2-HA3*) (**g**) treated with λ-phosphatase with or without phosphatase inhibitors. **b, h**, YJL934 (*cdc28-4 ORC6-HA3*) or YJL865 (*CDC28 ORC6-HA3*) grown at 23 °C were arrested in early S phase with hydroxyurea (HU) (after a pre-arrest in G1 with α-factor) then shifted to either 38 °C or kept at 23 °C for a further 3 h. **c**, Log phase YJL865 (*ORC6-HA3*) and YJL1394 (*orc6-4A-HA3*). **i**, Log phase YJL3155 (*ORC2*) and YJL1737 (*orc2-6A*). **d, j**, YJL865 (*ORC6-HA3*)

cells were released (time 0) from an α-factor arrest in G1 and samples taken every 10 min for analysis by immunoblot, FACS (to determine time of S phase), and budding index with 4,6-diamidino-2-phenylindole (DAPI) staining (to determine time of Start and mitosis). The 80-min time point in **j** is absent. **e, k**, YJL1937 (*dbf2-2 ORC0*) cells were grown at 37 °C for 150 min to arrest them in late mitosis, released from the arrest (time 0) by shifting them to 23 °C, and sampled every 10 min for immunoblot analysis. **f, l**, immunoblot of *ORC6-HA3* *cdc* strains arrested by growth at 37 °C for 2–3 h (until more than 95% have appropriate bud morphology); drug arrests were performed on YJL864 (*ORC6-HA3*) using α-factor, hydroxyurea or nocodazole (NOC).